LLMExplainer: Large Language Model based Bayesian Inference for Graph Explanation Generation

Jiaxing Zhang*1, Jiayi Liu*2, Dongsheng Luo3, Jennifer Neville24, Hua Wei5

¹New Jersey Institute of Technology, ²Purdue University, ³Florida International University, ⁴Microsoft Research, ⁵Arizona State University jz48@njit.edu, liu2861@purdue.edu, dluo@fiu.edu, neville@purdue.edu, hua.wei@asu.edu

Abstract

Recent studies seek to provide Graph Neural Network (GNN) interpretability via multiple unsupervised learning models. Due to the scarcity of datasets, current methods easily suffer from learning bias. To solve this problem, we embed a Large Language Model (LLM) as knowledge into the GNN explanation network to avoid the learning bias problem. We inject LLM as a Bayesian Inference (BI) module to mitigate learning bias. The efficacy of the BI module has been proven both theoretically and experimentally. We conduct experiments on both synthetic and real-world datasets. The innovation of our work lies in two parts: 1. We provide a novel view of the possibility of an LLM functioning as a Bayesian inference to improve the performance of existing algorithms; 2. We are the first to discuss the learning bias issues in the GNN explanation problem.

1 Introduction

Interpreting the decisions made by Graph Neural Networks (GNNs) (Scarselli et al., 2009) is crucial for understanding their underlying mechanisms and ensuring their reliability in various applications. As the application of GNNs expands to encompass graph tasks in social networks (Feng et al., 2023; Min et al., 2021), molecular structures (Chereda et al., 2019; Mansimov et al., 2019), traffic flows (Wang et al., 2020; Li and Zhu, 2021; Wu et al., 2019; Lei et al., 2022), and knowledge graphs (Sorokin and Gurevych, 2018), GNNs achieve state-of-the-art performance in tasks including node classification, graph classification, graph regression, and link prediction. The burgeoning demand highlights the necessity of enhancing GNN interpretability to strengthen model transparency and user trust, particularly in high-stakes settings (Yuan et al., 2022; Longa et al., 2022), and to facilitate insight extraction in complex fields

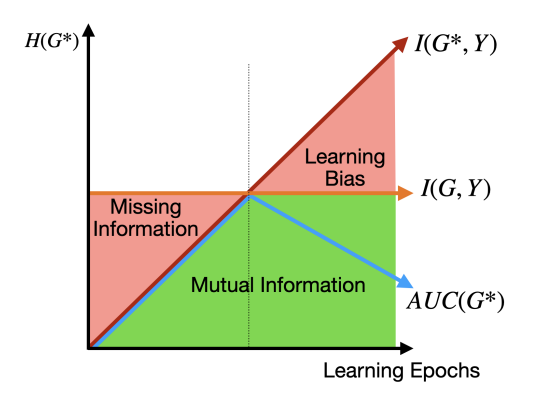


Figure 1: Intuitive visualization of learning bias.

such as healthcare and drug discovery (Zhang et al., 2022; Wu et al., 2022; Li et al., 2022).

Recent efforts in explaining GNN (Ying et al., 2019; Luo et al., 2020; Zhang et al., 2023b) have sought to enhance GNN interpretability through multiple learning objectives, with a particular focus on the graph information bottleneck (GIB) method. GIB's goal is to distill essential information from graphs for clearer model explanations. However, the effectiveness of GIB hinges on the availability of well-annotated datasets, which are instrumental in accurately training and validating these models. Unfortunately, such datasets are rare, primarily due to the significant expert effort required for accurate annotation and occasionally due to the inherent complexity of the graph data itself. This scarcity poses a serious challenge, leading to a risk of learning bias in explaining GNN. Learning bias arises when the model overly relies on the limited available data, potentially leading to incorrect or over-fitted interpretations. We illustrate this phenomenon in Fig. (1) and provide empirical evidence in Fig. (4).

As demonstrated in the figures, learning bias becomes increasingly problematic as the model continues to train on sparse data. Initially, the model might improve as it learns to correlate the

^{*}These authors contributed equally to this work.

sub-graph G^* with the label Y, optimizing mutual information $I(G^*,Y)$. However, beyond a certain point, keeping optimizing $I(G^*,Y)$ leads to an over-reliance on the limited and possibly non-representative data available, thereby aggravating the learning bias. This situation is depicted through the divergence of mutual information and actual performance metrics, such as AUC, where despite higher mutual information, the practical interpretability and accuracy of the model decline.

To mitigate the learning bias, current models often stop training early, a practice to prevent the exacerbation of learning bias. However, this approach is inherently flawed, especially in real-world applications lacking comprehensive validation datasets, leading potentially to under-fitting and inadequate model generalization. This emphasizes the need for innovative approaches to model training and interpretation that can navigate the challenges posed by sparse ground truth in explaining GNNs.

To address the challenges posed by sparse ground truth annotations and the consequent risk of learning bias in explaining GNNs, we propose LLMExplainer, a versatile GNN explanation framework that incorporates the insights from Large Language Model (LLM) into a wide array of backbone GNN explanation models, ranging from instance-level to model-level explanation models(Shan et al., 2021; Ying et al., 2019; Luo et al., 2020; Yuan et al., 2021; Spinelli et al., 2022; Wang et al., 2021b; Yuan et al., 2021; Shan et al., 2021; Chen et al., 2024). The LLMs act as a grader, and the evaluations from LLMs are then integrated into the model to inform a weighted gradient descent process. Specifically, to ensure a satisfactory level of explanation performance, we embed Bayesian Variational Inference into the original GNN explainers and use LLM as the prior knowledge in Bayesian Variational Inference. We prove that with the injection of LLM, LLMExplainer will mitigate the learning bias problem. Our experimental results show the effectiveness of enhancing the backbone explanation models with faster convergence and fortifying them against learning bias.

In summary, the main contributions of this paper are:

 We propose a new and general framework, LLMExplainer, which solves the problem of learning bias in the graph explanation process by embedding the Large Language Model into the graph explainer with a Bayesian inference process and improving the explanation accuracy.

- We theoretically prove the effectiveness of the proposed algorithm and show that the lower bound of LLMExplainer is no less than the original bound of baselines. Our proposed method achieved the best performance through five datasets compared to the baselines.
- We are the first to discuss this learning bias problem in the domain of graph explanation and provide the potential of the Large Language Model as a Bayesian inference module to benefit the current works.

2 Related Work

2.1 Graph Neural Networks and Graph Explanations

Graph neural networks (GNNs) are on the rise for analyzing graph structure data, as seen in recent research studies (Dai et al., 2022; Feng et al., 2023; Hamilton et al., 2017). There are two main types of GNNs: spectral-based approaches (Bruna et al., 2013; Kipf and Welling, 2016; Tang et al., 2019) and spatial-based approaches (Atwood and Towsley, 2016; Duvenaud et al., 2015; Xiao et al., 2021). Despite the differences, message passing is a common framework for both, using pattern extraction and message interaction between layers to update node embeddings. However, GNNs are still considered a black box model with a hard-tounderstand mechanism, particularly for graph data, which is harder to interpret compared to image data. To fully utilize GNNs, especially in high-risk applications, it is crucial to develop methods for understanding how they work.

Many attempts have been made to interpret GNN models and explain their predictions (Shan et al., 2021; Ying et al., 2019; Luo et al., 2020; Yuan et al., 2021; Spinelli et al., 2022; Wang et al., 2021b). These methods can be grouped into two categories based on granularity: (1) instance-level explanation, which explains the prediction for each instance by identifying significant substructures (Ying et al., 2019; Yuan et al., 2021; Shan et al., 2021), and (2) model-level explanation, which seeks to understand the global decision rules captured by the GNN (Luo et al., 2020; Spinelli et al., 2022; Baldassarre and Azizpour, 2019). From a methodological perspective, existing

methods can be classified as (1) self-explainable GNNs (Baldassarre and Azizpour, 2019; Dai and Wang, 2021), where the GNN can provide both predictions and explanations; and (2) post-hoc explanations (Ying et al., 2019; Luo et al., 2020; Yuan et al., 2021), which use another model or strategy to explain the target GNN. In this work, we focus on post-hoc instance-level explanations, which involve identifying instance-wise critical substructures to explain the prediction. Various strategies have been explored, including gradient signals, perturbed predictions, and decomposition.

Perturbed prediction-based methods are the most widely used in post-hoc instance-level explanations. The idea is to learn a perturbation mask that filters out non-important connections and identifies dominant substructures while preserving the original predictions. For example, GNNExplainer (Ying et al., 2019) uses end-to-end learned soft masks on node attributes and graph structure, while PG-Explainer (Luo et al., 2020) incorporates a graph generator to incorporate global information. RG-Explainer (Shan et al., 2021) uses reinforcement learning technology with starting point selection to find important substructures for the explanation.

2.2 Bayesian Inference

MacKay (1992) came up with the Bayesian Inference in general models, while Graves (2011) first applied Bayesian Inference to neural networks. Currently, Bayesian Inference has been applied broadly in computer vision (CV), nature language processing (NLP), etc (Müller et al., 2021; Gal and Ghahramani, 2015; Xue et al., 2021; Song et al., 2024).

Bayesian Variational techniques have seen extensive uptake in Bayesian approximate inference. They adeptly reframe the posterior inference challenge as an optimization endeavor (Wang et al., 2023). When compared to Markov Chain Monte Carlo, which is another Bayesian Inference method, Variational Inference exhibits enhanced convergence and scalability, making it better suited for tackling large-scale approximate inference tasks.

Due to the nature of Bayesian Variational Inference, it has been embedded into neural networks called Bayesian Neural Networks (Graves, 2011). A major drawback of current Deep Neural Networks is that they use fixed parameter values, and fail to provide uncertainty estimations, resulting in a limitation in uncertainty. BNNs are extensively used in fields like active learning, Bayesian

optimization, and bandit problems, as well as in out-of-distribution sample detection problems like anomaly detection and adversarial sample detection.

2.3 Large Language Model

Large Language Models (LLMs) have been widely used since 2023 (Bubeck et al., 2023; Brown et al., 2020; Zhou et al., 2022). Based on the architecture of Transformer(Vaswani et al., 2017), LLMs have achieved remarkable success in various Natural Language Processing (NLP) tasks. LLMs have spurred discussions from multiple angles, including LLM efficiency (Liu et al., 2024; Wan et al., 2024), personalized LLMs (Mysore et al., 2023; Fang et al., 2024), prompt engineering(Wei et al., 2022; Song et al., 2023), fine tuning(Lai et al., 2024), etc.

Beyond their traditional domain of NLP, LLMs have found extensive usage in diverse fields such as computer vision (Wang et al., 2024; Dang et al., 2024), graph learning (He et al., 2023), and recommendation systems (Jin et al., 2023; Wu et al., 2024), etc. By embedding LLMs into existing systems, researchers and practitioners have observed enhanced performance across various domains, underscoring the transformative impact of these models on modern AI applications.

3 Preliminary

3.1 Notations and Problem Definition

We summarize all the important notations in Table 3 in the appendix. We denote a graph as $G = (\mathcal{V}, \mathcal{E}; \boldsymbol{X}, \boldsymbol{A})$, where $\mathcal{V} = \{v_1, v_2, ..., v_n\}$ represents a set of n nodes and $\mathcal{E} \subseteq \mathcal{V} \times \mathcal{V}$ represents the edge set. Each graph has a feature matrix $\boldsymbol{X} \in \mathbb{R}^{n \times d}$ for the nodes. where in $\boldsymbol{X}, \boldsymbol{x}_i \in \mathbb{R}^{1 \times d}$ is the d-dimensional node feature of node v_i . \mathcal{E} is described by an adjacency matrix $\boldsymbol{A} \in \{0,1\}^{n \times n}$. $A_{ij} = 1$ means that there is an edge between node v_i and v_j ; otherwise, $A_{ij} = 0$.

For the graph classification task, each graph G has a ground-truth label $\bar{Y} \in \mathcal{C}$, with a GNN model f trained to classify G into its class, i.e., $f:(X,A)\mapsto \bar{Y}\in\{1,2,...,C\}$. For the node classification task, each graph G denotes a K-hop sub-graph centered around node v_i , with a GNN model f trained to predict the label for node v_i based on the node representation of v_i learned from G. Since the node classification can be converted to computation graph classification task (Ying et al.,

2019; Luo et al., 2020), we focus on the graph classification task in this work. For the graph regression task, each graph G has a label $\bar{Y} \in \mathbb{R}$, with a GNN model f trained to predict G into a regression value, i.e., $f: (X, A) \mapsto \bar{Y} \in \mathbb{R}$.

Informative feature selection has been well studied in non-graph structured data (Li et al., 2017), and traditional methods, such as concrete autoencoder (Balın et al., 2019), can be directly extended to explain features in GNNs. In this paper, we focus on discovering important typologies. Formally, the obtained explanation G^* is depicted by a binary mask $M \in \{0,1\}^{n \times n}$ on the adjacency matrix, e.g., $G^* = (\mathcal{V}, \mathcal{E}, A \odot M; X)$, \odot means elements-wise multiplication. The mask highlights components of G which are essential for f to make the prediction.

3.2 Graph Information Bottleneck

For a graph G follows the distribution with $P_{\mathcal{G}}$, we aim to get an explainer function $\hat{G}=g_{\alpha}(G)$, where α are the parameters of explanation generator g. To solve the graph information bottleneck, previous methods (Ying et al., 2019; Luo et al., 2020; Zhang et al., 2023b) are optimized under the following objective function:

$$G^* = \arg\min_{\hat{G}} I(G, \hat{G}) - \lambda I(Y, \hat{G}), \hat{G} \in \hat{\mathcal{G}}, (1)$$

where G^* is the optimized sub-graph explanation produced by optimized g, \hat{G} is the explanation candidate, and $\hat{\mathcal{G}} = \{\hat{G}\}$ is the set of \hat{G} observations. During the explaining procedure, this objective function would minimize the size constraint $I(G,\hat{G})$ and maximize the label mutual information $I(Y,\hat{G})$. λ is the hyper-parameter which controls the trade-off between two terms.

Since it is untractable to directly calculate the mutual information between prediction label Y and sub-graph explanation \hat{G} , to estimate the objective, Eq. (1) is approximated as

$$G^* = \arg\min_{\hat{G}} I(G, \hat{G}) - \lambda I(Y, f(\hat{G})), \hat{G} \in \hat{\mathcal{G}}.$$
(2)

Since G^* is generated by $g_{\alpha}(\cdot)$, instead of optimize \hat{G} , we optimize α^* with $h(\alpha,\lambda,G,f)=I(G,g_{\alpha}(G))-\lambda I(Y,f(g_{\alpha}(G)))$, then we have $\alpha^*=\arg\min h(\alpha,\lambda,G,f)$, where $I(Y,G^*)\sim I(Y,f(G^*))$ and f is the pre-trained GNN model.

4 Methodology

Fig. (2) presents an overview of the structure of LLMExplainer. The previous method is depicted

on the left, while LLMExplainer incorporates a Bayesian Variational Inference process into the entire architecture, utilizing a large language model as the grader. (In the previous explanation procedure, the explanation sub-graph is generated via an explanation model to explain the original graph and the to-be-explained prediction model. The explanation model is optimized by minimizing the size constraint $I(G, \hat{G})$ and maximizing the label mutual information $I(Y, \hat{Y})$, within $h(\alpha, \lambda, G, f)$, which is introduced in Section 3.2.

In our proposed framework, after generating the explanation sub-graph, we evaluate it through a Bayesian Variational Inference process, which is realized using a Large Language Model agent acting as a human expert. The enhanced explanation \hat{G} is then produced using Eq. (7). Note that, with the introduction of the Bayesian Variational Inference process, the previous distribution for α in $g_{\alpha}(\cdot)$ will shift to β in $g'_{\beta}(\cdot)$. Finally, we optimize the explanation model with new $I(G, \hat{G})$ and $I(Y, \hat{Y})$ within $h(\beta, \lambda, G, f)$. We provide detailed formulas for the LLM-based Bayesian Variational Inference in Section 4.1 and a detailed prompt-building procedure in Section 4.2. Our training procedure is provided in Algorithm. (1).

4.1 Bayesian Variational Inference In Explainer

The injection of Bayesian Variational Inference into the GNN Explainer helps mitigate the learning bias problem. In this section, we will provide details on how we achieve this goal and present a theoretical proof for our approach. We begin by injecting the knowledge learned from the LLM as a weighted score and adding the remaining objective with a graph noise. Instead of adopting weighted noise, or gradient noise(Neelakantan et al., 2015), we choose random Gaussian noise in this paper(Graves, 2011).

Problem 1 (Knowledge Enhanced Post-hoc Instance-level GNN Explanation). Given a trained GNN model f and a knowledgeable Large Language Model ϕ , for an arbitrary input graph $G = (\mathcal{V}, \mathcal{E}; \boldsymbol{X}, \boldsymbol{A})$, the goal of post-hoc instance-level GNN explanation is to find a sub-graph G^* with Bayesian Inference embedded explanation generator $g'_{\beta}(\cdot)$, that can explain the prediction of f on G with the Large Language Model grading $s = \phi(\hat{G}, G), s \in [0, 1]$ in circle, as $\hat{G} = g'_{\beta}(G) = sg_{\alpha}(G) + (1-s)G^{\mathcal{N}}, \beta^* = h(\beta, \lambda, G, f)$, where β is the parameter for $g'(\cdot)$ and g'_{β} is the explainer

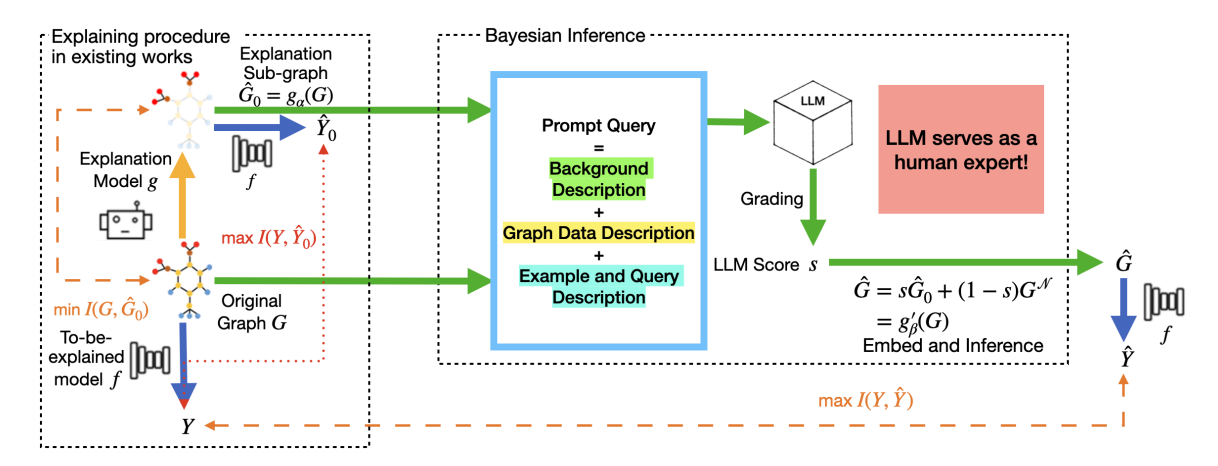


Figure 2: The architecture of our proposed framework for graph explaining and Bayesian inference on one graph sample in one epoch. \hat{G}_0 is the sub-graph explanation candidate before Bayesian inference and $\hat{Y}_0 = f(\hat{G}_0)$ is the prediction label for \hat{G}_0 . The explaining procedure in existing works on the left part optimizes the sub-graph explanation by minimizing the size constraint $I(G,\hat{G}_0)$ and maximizing the mutual information $I(Y,\hat{Y}_0)$, which would face the learning bias problem after epochs. We introduced the Bayesian inference together with the LLM, which serves as a human expert to produce the embedded graph \hat{G} and replace $I(Y,\hat{Y}_0)$ with $I(Y,\hat{Y})$ in the objective function, where $\hat{Y}=f(\hat{G})$ is the prediction label for \hat{G} . The detailed illustration of prompting is shown in Fig. (3).

model integrated with the Bayesian inference procedure.

The distribution of α and β will be different. Suppose we add the fitting score as a posterior knowledge. Then we will have the prior probability as $P(\hat{G}|\alpha)$, and the posterior probability as $Pr(\hat{G}|\alpha,s)$. With variational inference, suppose we approximates $Pr(\hat{G}|\alpha,s)$ over a class of tractable distributions Q, with $Q(\hat{G}|\beta)$, then the approximation becomes

$$G^* = \arg\min_{\hat{G}} \mathbb{E}_{\hat{G} \sim Q(\beta)} \left[-\ln \frac{Pr(s|\hat{G})P(\hat{G}|\alpha)}{Q(\hat{G}|\beta)} \right]$$
(3)

We denote the network loss $L(\hat{G}, s)$ as $L(\hat{G}, s) = -\ln Pr(s|\hat{G})$ (Graves, 2011), then we will have variational energy F as

$$F = \mathbb{E}_{\hat{G} \sim Q(\beta)} L(\hat{G}, s) + KL[Q(\beta)||P(\alpha)] \quad (4)$$

Definition 4.1. We define error loss $L^E(\beta, s)$ and complexity loss $L^C(\beta, s)$ in which

$$L^{E}(\beta, s) = \mathbb{E}_{\hat{G} \sim Q(\beta)} L(\hat{G}, s)$$

$$L^{C}(\beta, \alpha) = KL[Q(\beta)||P(\alpha)]$$
(5)

Then we will have

$$L(\alpha, \beta, s) = L^{E}(\beta, s) + L^{C}(\beta, \alpha) \tag{6}$$

where $L(\alpha, \beta, s)$ is the *Minimum Description* length form of variational energy F (Rissanen, 1978).

Hypothesis 1. We suppose that the s is accurate enough to estimate the fitting between \hat{G} and G. When $\hat{G} = G^*$, we have s = 1.

The hypothesis has been tested in Fig. (4). In the following theorem, we prove that the objective function is at least sub-optimal to avoid the learning bias with accurate s.

Theorem 1. When we reach the optimum $\hat{G} = G^*$, we will have the gradient $\Delta = \frac{\partial F}{\partial \hat{G}^*} \approx 0$, trapping G^* at the optimum point to avoid learning bias.

Proof. The generation of \hat{G} included two steps:

- 1. Generate from the original generator $g_{\alpha}(\cdot)$ with $\hat{G}_0 = g_{\alpha}(G)$.
- 2. Embed the fitting score with $\hat{G} = s\hat{G}_0 + (1 s)G^{\mathcal{N}}, G^{\mathcal{N}} \sim \mathcal{N}(0,1)$ where \hat{G} is the explanation sub-graph, s is the LLM score of \hat{G} with $s = \phi(\hat{G}, G), G^{\mathcal{N}}$ is the Gaussian noise.

Then we have the embedded inference network as

$$\hat{G} = g'_{\beta}(G) = sg_{\alpha}(G) + (1 - s)G^{\mathcal{N}}$$
 (7)

The distribution of \hat{G} is denoted as Q, where $\hat{G} \sim Q(\beta)$. Then we can calculate $L^E(\beta,s)$ and $L^C(\beta,\alpha)$ in Eq. (5) separately. We will discuss the scenarios of error loss $L^E(\beta,s)$ and network loss $L^C(\beta,\alpha)$ when we have $\hat{G}=G^*$ and $s\to 1$.

$$L^{E}(\beta, s) = \mathbb{E}_{\hat{G} \sim Q(\beta)} L(\hat{G}, s)$$
$$= -\int P(\hat{G}|\beta) \cdot \ln Pr(s|\hat{G}) d\hat{G}. \tag{8}$$

Prompt Query Here are some examples: \n < EXAMPLE I will give you a graph 'G' and a The graph is represented by explanation sub-graph 'Ge'. \n edge index and node SHOT1> \n < EXAMPLE SHOT2> \n <GNN TASK DESCRIPTION> \n features. Edge index Now, I'm giving you the graph 'G' and sub-Your task is grading the given explanation graph 'Ge': \n contains the list source The graph 'G' is: """<GRAPH SEQ>""" \n sub-graph 'Ge' for given original graph 'G nodes and targets nodes in The sub-graph 'Ge' is: """<GRAPH SEQ>" regarding its correctness and the graph as [[node_id_src, completeness \n node_id_tat]]; Node features The grade scores are in <GRADE dictionary contains the node Please grade the sub-graph 'Ge'. \n LEVELS>, higher the score is, better the features as {node_id: REMEMBER IT: Keep your answer short! sub-graph 'Gs' is. \n feature} \n **Background Description Graph Data Description Example and Query Description**

Placeholder	Description	
<gnn description="" task=""></gnn>	A task-specific description to help LLM agent understand the graph task.	
<grade levels=""></grade>	A range of candidate scores for the LLM agent to choose from.	
<graph seq=""></graph>	A sequence consists of the edge index and node features of a graph sample.	
<example shot=""></example>	An example to teach LLM how to grade the explanation candidates.	

Figure 3: The prompt construction of LLMExplainer in Bayesian Variational Inference Process. For an original graph G and sub-graph explanation candidate \hat{G} , namely 'G' and 'Ge' in text, Large Language Models could tackle and reason the graph tasks with commonsense and expert knowledge, then grade the explanation candidate sub-graph. The placeholders would be replaced with the full text during prompting. Their usage is shown in the table.

When
$$s \to 1$$
, we have $L^{E}(\beta, s) \stackrel{s \to 1}{\approx} -\int sP(\hat{G}_{0}|\alpha) \cdot \ln Pr\left(s|\hat{G}_{0}\right) d\hat{G}_{0}$.

$$L^{C}(\beta, \alpha) \sim KL[sg_{\alpha}(G) + (1-s)G^{\mathcal{N}}||g_{\alpha}(G)]$$

$$= \int (s\hat{G}_{0} + (1-s)G^{\mathcal{N}})$$

$$\log \left(\frac{s\hat{G}_{0} + (1-s)G^{\mathcal{N}}}{\hat{G}_{0}}\right) d\hat{G}_{0}.$$
(9)

When $s \to 1$, $\frac{1-s}{s} \frac{G^{\mathcal{N}}}{\hat{G}_0} \to 0$, we have $L^C(\beta, \alpha) \stackrel{s \to 1}{\approx} (1-s)(G^{\mathcal{N}} - \hat{G}_0)d\hat{G}_0$.

With Eq. (6), when \hat{G}_0 is optimal and $s \to 1$, we have

$$\Delta = \frac{\partial F}{\partial \hat{G}_0} = -sP(\hat{G}_0|\alpha) \cdot \ln Pr\left(s|\hat{G}_0\right) + (1-s)(G^{\mathcal{N}} - \hat{G}_0)$$

Based on Hypothesis 1, we have $Pr(s|\hat{G}_0) \to 1$, $\Delta \approx 0$. Hence, when we reach the optimum subgraph G^* , our algorithm will trap the optimum with the gradient $\Delta \to 0$ to mitigate learning bias. Due to page limitations, we present the full proof in the Appendix. \square

4.2 Prompting

As shown in Fig. (3), we build a pair (G, \hat{G}) into a prompt. It contains several parts: (1). We provide a background description for the task. **<GNN TASK DESCRIPTION>** is a task-specific description. For example: for dataset BA-Motif-Counting,

it would be "The ground truth explanation subgraph 'Ge' of the original graph 'G' is a circle motif."; for chemical dataset MUTAG, it would be "The ground truth explanation sub-graph 'Ge' of the original graph 'G' is sub-compound and decides the molecular property of mutagenicity on Salmonella Typhimurium." <GRADE LEVELS> is a range of candidate scores according to the task, e.g.: [0,1]. (2). We describe how we express a graph in text, which would help the LLM understand our graph sample. The **<GRAPH SEQ>** contains two parts: edge index and node features, which transport the graph-structure data into text, e.g.:edge index: [[0, 1], [1, 2], [2, 0]], node feature: $\{0: [3.6], 1: [2.4], 2: [9.9]\}$. (3). We then provide a few shots to the LLM. The **<EXAMPLE** SHOT> contains several pairs of to-be-grade candidates and their corresponding grades. We ask the LLM to grade our query candidate. (4). Finally, we regularize the answer of LLM to be a single number with the "REMEMBER IT: Keep your answer short!" prompt. We put the complete samples in the GitHub repository along with our code and data.

5 Experimental Study

We conduct comprehensive experimental studies on benchmark datasets to empirically verify the effectiveness of the proposed LLMExplainer. Specifically, we aim to answer the following research questions:

(10)

Table 1: Explanation faithfulness in terms of AUC-ROC on edges under five datasets. The higher, the better. Our proposed method achieves consistent improvements over the backbone GIB-based explanation method and other baselines.

	Graph Classification			Graph Regression	
	MUTAG	Fluoride-Carbonyl	Alkane-Carbonyl	BA-Motif-Volume	BA-Motif-Counting
GRAD	$0.573_{\pm 0.000}$	$0.604_{\pm 0.000}$	$0.496_{\pm 0.000}$	$0.418_{\pm 0.000}$	$0.516_{\pm 0.000}$
ReFine	$0.612_{\pm 0.004}$	$0.507_{\pm 0.003}$	$0.630_{\pm 0.007}$	$0.572_{\pm 0.006}$	$0.742_{\pm 0.011}$
GNNExplainer	$0.682_{\pm 0.009}$	$0.540_{\pm 0.002}$	$0.532_{\pm 0.008}$	$0.501_{\pm 0.009}$	$0.504_{\pm0.003}$
PGExplainer	$0.601_{\pm 0.151}$	$0.512_{\pm 0.010}$	$0.586_{\pm0.031}$	$0.547_{\pm 0.040}$	$0.969_{\pm 0.017}$
+ LLM	$0.763_{\pm 0.106}$	$0.719_{\pm 0.017}$	$0.791_{\pm 0.003}$	$0.979_{\pm 0.009}$	$0.990_{\pm 0.004}$
(improvement)	+0.162	+0.207	+0.205	+0.432	+0.021

- RQ1: Could the proposed framework outperform the baselines in identifying the explanation sub-graphs for the to-be-explained GNN model?
- RQ2: Could the LLM score help address the learning bias issue?
- RQ3: Could the LLM score reflect the performance of the explanation sub-graph; is it effective in the proposed method?

5.1 Experiment Settings

To evaluate the performance of LLMExplainer, we use five benchmark datasets with groundtruth explanations. These include two synthetic graph regression datasets: BA-Motif-Volume and BA-Motif-Counting (Zhang et al., 2023a), with three real-world datasets: MUTAG (Kazius et al., 2005), Fluoride-Carbonyl (Sanchez-Lengeling et al., 2020), and Alkane-Carbonyl (Sanchez-Lengeling et al., 2020). We take GRAD (Ying et al., 2019), GNNExplainer (Ying et al., 2019), ReFine (Wang et al., 2021a), and PGExplainer (Luo et al., 2020) for comparison. Specifically, we pick PGExplainer as a backbone and apply LLMExplainer to it. We follow the experimental setting in previous works (Ying et al., 2019; Luo et al., 2020; Sanchez-Lengeling et al., 2020; Zhang et al., 2023b) to train a Graph Convolutional Network (GCN) model with three layers. We use GPT-3.5 as our LLM grader for the explanation candidates. To evaluate the quality of explanations, we approach the explanation task as a binary classification of edges. Edges that are part of ground truth sub-graphs are labeled as positive, while all others are deemed negative. We take the importance weights given by the explanation methods as prediction scores. An effective explanation technique should be able to assign higher weights to the edges within the ground truth sub-graphs compared to those outside of them. We utilize the

AUC-ROC metric(\(\epsilon\)) for quantitative evaluation. *.

5.2 Quantitative Evaluation (RQ1)

In this section, we compare our proposed method, LLMExplainer, to other baselines. Each experiment was conducted 10 times using random seeds from 0 to 9, with 100 epochs, and the average AUC scores as well as standard deviations are presented in Table 1. The results demonstrate that LLMExplainer provides the most accurate explanations among several baselines. Specifically, it improves the AUC scores by an average of 0.227/42.5% on synthetic datasets and 0.191/34.1% on real-world datasets. In dataset BA-Motif-Volume, we achieve 0.432/79.0% improvement compared to the PGExplainer baseline. The reason is there is serious learning bias with PG-Explainer on BA-Motif-Volume, which is shown in Fig. (4). The performance improvement in BA-Motif-Volume is not significant because of (1). the learning bias in this dataset is specifically slight; (2). The PGExplainer is well-trained at the epoch 100. Comparisons with baseline methods highlight the advantage of Bayesian inference and LLM serving as a knowledge agent in training.

5.3 Qualitative Evaluation (RQ2)

As shown in Fig. (4), we visualize the training procedure of PGExplainer and LLMExplainer on five datasets. The first row is PGExplainer and the second row is LLMExplainer. From left to right, the five datasets are MUTAG, Fluoride-Carbonyl, Alkane-Carbonyl, BA-Motif-Volume, and BA-Motif-Counting respectively. We visualize and compare the AUC performance, LLM score, and train loss of them. Additionally, the LLM score is not used in PGExplainer, we retrieve it with the explanation candidates during training. As we can observe in the BA-Motif-Volume dataset, the AUC perfor-

^{*}Our data and code are available at: https://anonymous. 4open.science/r/LLMExplainer-A4A4

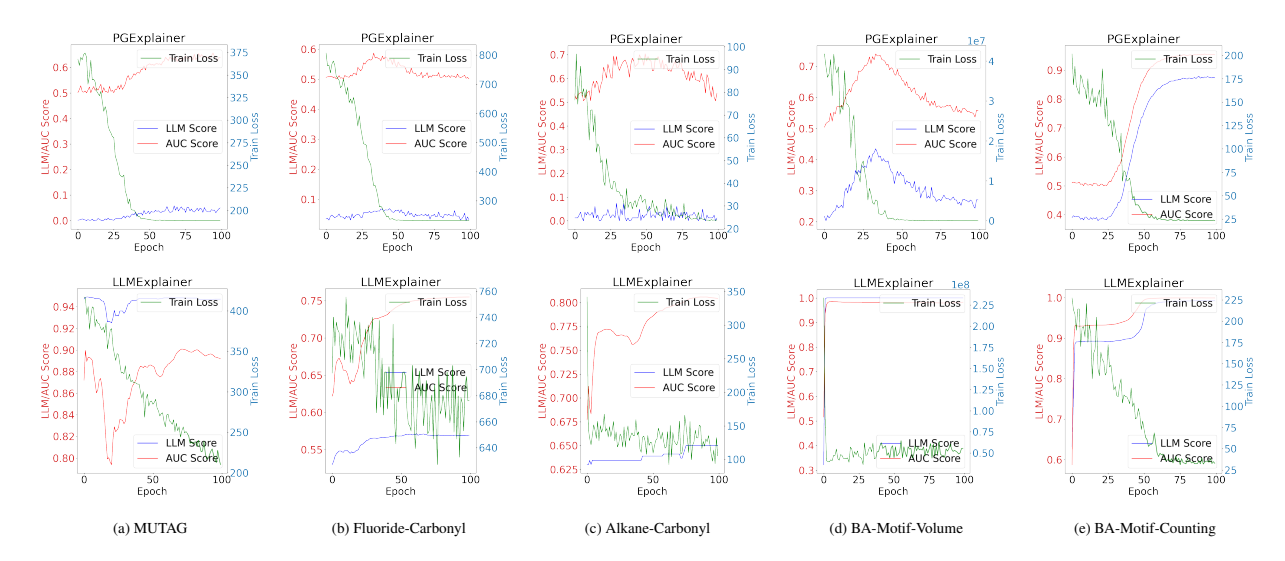


Figure 4: Visualization of AUC, LLM Score, and Training Loss curve by training epochs. We choose one seed for each explainer on each dataset.

	MUTAG	Fluoride-Carbonyl	Alkane-Carbonyl	BA-Motif-Volume	BA-Motif-Counting
Random Score	$0.456_{\pm0.280}$	$0.601_{\pm 0.058}$	$0.683_{\pm 0.092}$	$0.798_{\pm 0.111}$	$0.887_{\pm 0.146}$
LLM Score	$0.763_{\pm 0.106}$	$0.719_{\pm 0.017}$	$0.791_{\pm 0.003}$	$0.979_{\pm 0.009}$	$0.990_{\pm 0.004}$

Table 2: Ablation study on the effectiveness of the LLM score. The results in the table compare the performance of the proposed method with the LLM score and random score.

mance and LLM score increase in the first 40 epochs. However, they drop persistently to around 0.5/0.3 after 100 epochs, indicating a learning bias problem. For LLMExplainer, based on PGExplainer, on the second row, we can observe that the AUC performance and LLM Score increase to 0.9+ and maintain themselves stably. This observation is similar in Fluoride-Carbonyl and Alkane-Carbonyl datasets. The LLM score slightly dropped at around epoch 40 and then recovered. The results show that our proposed framework LLMExplainer could effectively alleviate the learning bias problem during the explaining procedure.

5.4 Ablation Study (RQ3)

In this section, we conduct the experiments on the ablation study of the LLMExplainer. When we have the LLM score, we may be concerned about whether or not this score could reflect the real performance of the explanation sub-graph candidates and whether it would work for the proposed framework. So, we compare the performance of the framework with the LLM score and random score. In the model with the random score, we replace the LLM grading module with a random number generator. As shown in Table 2, the results show that the LLM score could effectively enhance the Bayesian Inference procedure in explaining.

6 Conclusion

In this work, we proposed LLMExplainer, which incorporated the graph explaining the procedure with Bayesian Inference and the Large Language Model. We build the to-be-explained graph and the explanation candidate into the prompt and take advantage of the Large Language Model to grade the candidate. Then we use this score in the Bayesian Inference procedure. We conduct experiments on three real-world graph classification tasks and two synthetic graph regression tasks to demonstrate the effectiveness of our framework. By comparing the baselines and PGExplainer as the backbone, the results show the advantage of our proposed framework. Further experiments show that the LLM score is effective in the whole pipeline.

7 Limitations

While we acknowledge the effectiveness of our method, we also recognize its limitations. Specifically, although our approach theoretically and empirically proves the benefits of integrating the LLM agent into the explainer framework, the scope of the datasets and Large Language Models remains limited. To address this challenge, we plan to explore more real-world datasets and deploy additional LLMs for a more comprehensive evaluation in the future work.

References

- James Atwood and Don Towsley. 2016. Diffusion-convolutional neural networks. *Advances in neural information processing systems*, 29.
- Federico Baldassarre and Hossein Azizpour. 2019. Explainability techniques for graph convolutional networks. *arXiv preprint*.
- Muhammed Fatih Balın, Abubakar Abid, and James Zou. 2019. Concrete autoencoders: Differentiable feature selection and reconstruction. In *International conference on machine learning*, pages 444–453. PMLR.
- Tom Brown, Benjamin Mann, Nick Ryder, Melanie Subbiah, Jared D Kaplan, Prafulla Dhariwal, Arvind Neelakantan, Pranav Shyam, Girish Sastry, Amanda Askell, et al. 2020. Language models are few-shot learners. *Advances in neural information processing systems*, 33:1877–1901.
- Joan Bruna, Wojciech Zaremba, Arthur Szlam, and Yann LeCun. 2013. Spectral networks and locally connected networks on graphs. *arXiv preprint arXiv:1312.6203*.
- Sébastien Bubeck, Varun Chandrasekaran, Ronen Eldan, Johannes Gehrke, Eric Horvitz, Ece Kamar, Peter Lee, Yin Tat Lee, Yuanzhi Li, Scott Lundberg, et al. 2023. Sparks of artificial general intelligence: Early experiments with gpt-4. *arXiv preprint arXiv:2303.12712*.
- Zhuomin Chen, Jiaxing Zhang, Jingchao Ni, Xiaoting Li, Yuchen Bian, Md Mezbahul Islam, Ananda Mohan Mondal, Hua Wei, and Dongsheng Luo. 2024. Generating in-distribution proxy graphs for explaining graph neural networks. *Preprint*, arXiv:2402.02036.
- Hryhorii Chereda, Annalen Bleckmann, Frank Kramer, Andreas Leha, and Tim Beissbarth. 2019. Utilizing molecular network information via graph convolutional neural networks to predict metastatic event in breast cancer. In *GMDS*, pages 181–186.
- Enyan Dai, Wei Jin, Hui Liu, and Suhang Wang. 2022. Towards robust graph neural networks for noisy graphs with sparse labels. In *Proceedings of the Fifteenth ACM International Conference on Web Search and Data Mining*, pages 181–191.
- Enyan Dai and Suhang Wang. 2021. Towards self-explainable graph neural network. *arXiv preprint*.
- Bo Dang, Wenchao Zhao, Yufeng Li, Danqing Ma, Qixuan Yu, and Elly Yijun Zhu. 2024. Real-time pill identification for the visually impaired using deep learning.
- David K Duvenaud, Dougal Maclaurin, Jorge Iparraguirre, Rafael Bombarell, Timothy Hirzel, Alán Aspuru-Guzik, and Ryan P Adams. 2015. Convolutional networks on graphs for learning molecular fingerprints. *Advances in neural information processing systems*, 28.

- Chenhao Fang, Xiaohan Li, Zezhong Fan, Jianpeng Xu, Kaushiki Nag, Evren Korpeoglu, Sushant Kumar, and Kannan Achan. 2024. Llm-ensemble: Optimal large language model ensemble method for e-commerce product attribute value extraction. *arXiv preprint arXiv:2403.00863*.
- Zhiyuan Feng, Kai Qi, Bin Shi, Hao Mei, Qinghua Zheng, and Hua Wei. 2023. Deep evidential learning in diffusion convolutional recurrent neural network.
- Yarin Gal and Zoubin Ghahramani. 2015. Bayesian convolutional neural networks with bernoulli approximate variational inference. *arXiv preprint arXiv:1506.02158*.
- Alex Graves. 2011. Practical variational inference for neural networks. *Advances in neural information processing systems*, 24.
- Will Hamilton, Zhitao Ying, and Jure Leskovec. 2017. Inductive representation learning on large graphs. *Advances in neural information processing systems*, 30.
- Xiaoxin He, Xavier Bresson, Thomas Laurent, Adam Perold, Yann LeCun, and Bryan Hooi. 2023. Harnessing explanations: Llm-to-lm interpreter for enhanced text-attributed graph representation learning. In *The Twelfth International Conference on Learning Representations*.
- Ming Jin, Shiyu Wang, Lintao Ma, Zhixuan Chu, James Y Zhang, Xiaoming Shi, Pin-Yu Chen, Yuxuan Liang, Yuan-Fang Li, Shirui Pan, et al. 2023. Timellm: Time series forecasting by reprogramming large language models. *arXiv preprint arXiv:2310.01728*.
- Jeroen Kazius, Ross McGuire, and Roberta Bursi. 2005. Derivation and validation of toxicophores for mutagenicity prediction. *Journal of medicinal chemistry*, 48(1):312–320.
- Thomas N Kipf and Max Welling. 2016. Semisupervised classification with graph convolutional networks. *arXiv preprint arXiv:1609.02907*.
- Zhixin Lai, Xuesheng Zhang, and Suiyao Chen. 2024. Adaptive ensembles of fine-tuned transformers for llm-generated text detection. *arXiv* preprint *arXiv*:2403.13335.
- Xiaoliang Lei, Hao Mei, Bin Shi, and Hua Wei. 2022. Modeling network-level traffic flow transitions on sparse data. In *Proceedings of the 28th ACM SIGKDD Conference on Knowledge Discovery and Data Mining*, pages 835–845.
- Jundong Li, Kewei Cheng, Suhang Wang, Fred Morstatter, Robert P. Trevino, Jiliang Tang, and Huan Liu. 2017. Feature selection: A data perspective. *ACM Comput. Surv.*, 50(6).
- Mengzhang Li and Zhanxing Zhu. 2021. Spatial-temporal fusion graph neural networks for traffic flow forecasting. *Proceedings of the AAAI Conference on Artificial Intelligence*, 35(5):4189–4196.

- Yiqiao Li, Jianlong Zhou, Sunny Verma, and Fang Chen. 2022. A survey of explainable graph neural networks: Taxonomy and evaluation metrics. *arXiv preprint arXiv:2207.12599*.
- Jiayi Liu, Tinghan Yang, and Jennifer Neville. 2024. Cliqueparcel: An approach for batching llm prompts that jointly optimizes efficiency and faithfulness. *arXiv preprint arXiv:2402.14833*.
- Antonio Longa, Steve Azzolin, Gabriele Santin, Giulia Cencetti, Pietro Liò, Bruno Lepri, and Andrea Passerini. 2022. Explaining the explainers in graph neural networks: a comparative study. *arXiv preprint arXiv:2210.15304*.
- Dongsheng Luo, Wei Cheng, Dongkuan Xu, Wenchao Yu, Bo Zong, Haifeng Chen, and Xiang Zhang. 2020. Parameterized explainer for graph neural network. *Advances in neural information processing systems*, 33:19620–19631.
- David JC MacKay. 1992. Bayesian interpolation. *Neural computation*, 4(3):415–447.
- E. Mansimov, O. Mahmood, and S. Kang. 2019. Molecular geometry prediction using a deep generative graph neural network.
- Shengjie Min, Zhan Gao, Jing Peng, Liang Wang, Ke Qin, and Bo Fang. 2021. Stgsn a spatial—temporal graph neural network framework for time-evolving social networks. *Knowledge-Based Systems*, 214:106746.
- Samuel Müller, Noah Hollmann, Sebastian Pineda Arango, Josif Grabocka, and Frank Hutter. 2021. Transformers can do bayesian inference. *arXiv* preprint arXiv:2112.10510.
- Sheshera Mysore, Zhuoran Lu, Mengting Wan, Longqi Yang, Steve Menezes, Tina Baghaee, Emmanuel Barajas Gonzalez, Jennifer Neville, and Tara Safavi. 2023. Pearl: Personalizing large language model writing assistants with generation-calibrated retrievers. *arXiv* preprint arXiv:2311.09180.
- Arvind Neelakantan, Luke Vilnis, Quoc V Le, Ilya Sutskever, Lukasz Kaiser, Karol Kurach, and James Martens. 2015. Adding gradient noise improves learning for very deep networks. *arXiv preprint arXiv:1511.06807*.
- Jorma Rissanen. 1978. Modeling by shortest data description. Automatica, 14(5):465–471.
- Benjamin Sanchez-Lengeling, Jennifer Wei, Brian Lee, Emily Reif, Peter Wang, Wesley Qian, Kevin McCloskey, Lucy Colwell, and Alexander Wiltschko. 2020. Evaluating attribution for graph neural networks. *Advances in neural information processing systems*, 33:5898–5910.
- Franco Scarselli, Marco Gori, Ah Chung Tsoi, Markus Hagenbuchner, and Gabriele Monfardini. 2009. The graph neural network model. *IEEE Transactions on Neural Networks*, 20(1):61–80.

- Caihua Shan, Yifei Shen, Yao Zhang, Xiang Li, and Dongsheng Li. 2021. Reinforcement learning enhanced explainer for graph neural networks. In *Advances in Neural Information Processing Systems*.
- Xingchen Song, Di Wu, Binbin Zhang, Zhendong Peng, Bo Dang, Fuping Pan, and Zhiyong Wu. 2023. Zero-Prompt: Streaming Acoustic Encoders are Zero-Shot Masked LMs. In *Proc. INTERSPEECH 2023*, pages 1648–1652.
- Yizhi Song, Zhifei Zhang, Zhe Lin, Scott Cohen, Brian Price, Jianming Zhang, Soo Ye Kim, He Zhang, Wei Xiong, and Daniel Aliaga. 2024. Imprint: Generative object compositing by learning identity-preserving representation. *arXiv* preprint arXiv:2403.10701.
- Daniil Sorokin and Iryna Gurevych. 2018. Modeling semantics with gated graph neural networks for knowledge base question answering. In *Proceedings of the 27th International Conference on Computational Linguistics*, pages 3306–3317, Santa Fe, New Mexico, USA. Association for Computational Linguistics.
- Indro Spinelli, Simone Scardapane, and Aurelio Uncini. 2022. A meta-learning approach for training explainable graph neural networks. *IEEE Transactions on Neural Networks and Learning Systems*.
- Shanshan Tang, Bo Li, and Haijun Yu. 2019. Chebnet: Efficient and stable constructions of deep neural networks with rectified power units using chebyshev approximations. *arXiv* preprint arXiv:1911.05467.
- Ashish Vaswani, Noam Shazeer, Niki Parmar, Jakob Uszkoreit, Llion Jones, Aidan N Gomez, Łukasz Kaiser, and Illia Polosukhin. 2017. Attention is all you need. *Advances in neural information processing systems*, 30.
- Mengting Wan, Tara Safavi, Sujay Kumar Jauhar, Yujin Kim, Scott Counts, Jennifer Neville, Siddharth Suri, Chirag Shah, Ryen W White, Longqi Yang, et al. 2024. Tnt-llm: Text mining at scale with large language models. arXiv preprint arXiv:2403.12173.
- Chen Wang, Xu Wu, Ziyu Xie, and Tomasz Kozlowski. 2023. Scalable inverse uncertainty quantification by hierarchical bayesian modeling and variational inference. *Energies*, 16(22):7664.
- Wenhai Wang, Zhe Chen, Xiaokang Chen, Jiannan Wu, Xizhou Zhu, Gang Zeng, Ping Luo, Tong Lu, Jie Zhou, Yu Qiao, et al. 2024. Visionllm: Large language model is also an open-ended decoder for vision-centric tasks. *Advances in Neural Information Processing Systems*, 36.
- Xiang Wang, Ying-Xin Wu, An Zhang, Xiangnan He, and Tat-Seng Chua. 2021a. Towards multi-grained explainability for graph neural networks. In Advances in Neural Information Processing Systems 34: Annual Conference on Neural Information Processing Systems 2021, NeurIPS 2021, December 6-14, 2021, virtual, pages 18446–18458.

- Xiang Wang, Yingxin Wu, An Zhang, Xiangnan He, and Tat-seng Chua. 2021b. Causal screening to interpret graph neural networks.
- Xiaoyang Wang, Yao Ma, Yiqi Wang, Wei Jin, Xin Wang, Jiliang Tang, Caiyan Jia, and Jian Yu. 2020. Traffic flow prediction via spatial temporal graph neural network. In *Proceedings of The Web Conference* 2020, WWW '20, page 1082–1092, New York, NY, USA. Association for Computing Machinery.
- Jason Wei, Xuezhi Wang, Dale Schuurmans, Maarten Bosma, Fei Xia, Ed Chi, Quoc V Le, Denny Zhou, et al. 2022. Chain-of-thought prompting elicits reasoning in large language models. Advances in neural information processing systems, 35:24824–24837.
- Bingzhe Wu, Jintang Li, Junchi Yu, Yatao Bian, Hengtong Zhang, CHaochao Chen, Chengbin Hou, Guoji Fu, Liang Chen, Tingyang Xu, et al. 2022. A survey of trustworthy graph learning: Reliability, explainability, and privacy protection. *arXiv* preprint *arXiv*:2205.10014.
- Jing Wu, Suiyao Chen, Qi Zhao, Renat Sergazinov, Chen Li, Shengjie Liu, Chongchao Zhao, Tianpei Xie, Hanqing Guo, Cheng Ji, et al. 2024. Switchtab: Switched autoencoders are effective tabular learners. In *Proceedings of the AAAI Conference on Artificial Intelligence*, volume 38, pages 15924–15933.
- Zonghan Wu, Shirui Pan, Guodong Long, Jing Jiang, and Chengqi Zhang. 2019. Graph wavenet for deep spatial-temporal graph modeling. In *Proceedings of the 28th International Joint Conference on Artificial Intelligence*, IJCAI'19, page 1907–1913. AAAI
- Teng Xiao, Zhengyu Chen, Donglin Wang, and Suhang Wang. 2021. Learning how to propagate messages in graph neural networks. In *Proceedings of the 27th ACM SIGKDD Conference on Knowledge Discovery & Data Mining*, pages 1894–1903.
- Boyang Xue, Jianwei Yu, Junhao Xu, Shansong Liu, Shoukang Hu, Zi Ye, Mengzhe Geng, Xunying Liu, and Helen Meng. 2021. Bayesian transformer language models for speech recognition. In *ICASSP* 2021-2021 IEEE International Conference on Acoustics, Speech and Signal Processing (ICASSP), pages 7378–7382. IEEE.
- Zhitao Ying, Dylan Bourgeois, Jiaxuan You, Marinka Zitnik, and Jure Leskovec. 2019. Gnnexplainer: Generating explanations for graph neural networks. *Advances in neural information processing systems*, 32.
- Hao Yuan, Haiyang Yu, Shurui Gui, and Shuiwang Ji. 2022. Explainability in graph neural networks: A taxonomic survey. *IEEE Transactions on Pattern Analysis and Machine Intelligence*.
- Hao Yuan, Haiyang Yu, Jie Wang, Kang Li, and Shuiwang Ji. 2021. On explainability of graph neural networks via subgraph explorations. In *International Conference on Machine Learning*, pages 12241–12252. PMLR.

- He Zhang, Bang Wu, Xingliang Yuan, Shirui Pan, Hanghang Tong, and Jian Pei. 2022. Trustworthy graph neural networks: Aspects, methods and trends. *arXiv* preprint arXiv:2205.07424.
- Jiaxing Zhang, Zhuomin Chen, Hao Mei, Dongsheng Luo, and Hua Wei. 2023a. Regexplainer: Generating explanations for graph neural networks in regression task. *Preprint*, arXiv:2307.07840.
- Jiaxing Zhang, Dongsheng Luo, and Hua Wei. 2023b. Mixupexplainer: Generalizing explanations for graph neural networks with data augmentation. In *Proceed*ings of the 29th ACM SIGKDD Conference on Knowledge Discovery and Data Mining, KDD '23, page 3286–3296, New York, NY, USA. Association for Computing Machinery.
- Yongchao Zhou, Andrei Ioan Muresanu, Ziwen Han, Keiran Paster, Silviu Pitis, Harris Chan, and Jimmy Ba. 2022. Large language models are human-level prompt engineers. *arXiv preprint arXiv:2211.01910*.

8 Appendix

8.1 Error loss $L^E(\beta, s)$

The full proof of Equation 8 towards the error loss $L^E(\beta,s)$ is

$$\begin{split} L^E(\beta,s) &= \mathbb{E}_{\hat{G} \sim \, Q(\beta)} L(\hat{G},s) \\ &= -\int P(\hat{G}|\beta) \cdot \ln Pr(s|\hat{G}) d\hat{G} \\ \text{When } s \to 1 \text{, then we have} \\ &\stackrel{s \to 1}{\approx} -\int P(\hat{G}|\alpha) \cdot \ln Pr(s|\hat{G}) d\hat{G} \\ &= -\int sP(\hat{G}_0|\alpha) \cdot \\ &\ln Pr\left(s|s\hat{G}_0 + (1-s)G^{\mathcal{N}}\right) d\hat{G}_0 \\ &= -\int sP(\hat{G}_0|\alpha) \cdot \ln Pr\left(s|\hat{G}_0\right) d\hat{G}_0 \end{split}$$

8.2 Network loss $L^C(\beta, \alpha)$

The full proof of Equation 9 towards the network loss $L^C(\beta, \alpha)$ is

$$\begin{split} L^{C}(\beta,\alpha) &\sim KL[sg_{\alpha}(G) + (1-s)G^{\mathcal{N}}||g_{\alpha}(G)] \\ &= \int (s\hat{G}_{0} + (1-s)G^{\mathcal{N}}) \log \left(\frac{s\hat{G}_{0} + (1-s)G^{\mathcal{N}}}{\hat{G}_{0}}\right) d\hat{G}_{0} \\ &= \int (s\hat{G}_{0} + (1-s)G^{\mathcal{N}}) \log \left(s + (1-s)\frac{G^{\mathcal{N}}}{\hat{G}_{0}}\right) d\hat{G}_{0} \\ &= \int (s\hat{G}_{0} + (1-s)G^{\mathcal{N}}) \log s \left(1 + \frac{1-s}{s}\frac{G^{\mathcal{N}}}{\hat{G}_{0}}\right) d\hat{G}_{0} \\ &= \int (s\hat{G}_{0} + (1-s)G^{\mathcal{N}}) \left(\log s + \log\left(1 + \frac{1-s}{s}\frac{G^{\mathcal{N}}}{\hat{G}_{0}}\right)\right) d\hat{G}_{0} \\ &= \int (s\hat{G}_{0} + (1-s)G^{\mathcal{N}}) \left(\log s + \log\left(1 + \frac{1-s}{s}\frac{G^{\mathcal{N}}}{\hat{G}_{0}}\right)\right) d\hat{G}_{0} \\ &= \int (s\hat{G}_{0} + (1-s)G^{\mathcal{N}}) \left(\log s + \frac{1-s}{s}\frac{G^{\mathcal{N}}}{\hat{G}_{0}}\right) d\hat{G}_{0} \\ &= \int s\hat{G}_{0} \left(\log s + \frac{1-s}{s}\frac{G^{\mathcal{N}}}{\hat{G}_{0}}\right) d\hat{G}_{0} \\ &= \int s\hat{G}_{0} \log s + (1-s)G^{\mathcal{N}} d\hat{G}_{0} \\ &= \int s\hat{G}_{0} \log s + (1-s)G^{\mathcal{N}} d\hat{G}_{0} \\ &= \int (1-s)\hat{G}_{0} + (1-s)G^{\mathcal{N}} d\hat{G}_{0} \\ &= \int (1-s)\hat{G}_{0} + (1-s)G^{\mathcal{N}} d\hat{G}_{0} \\ &= \int (1-s)(G^{\mathcal{N}} - \hat{G}_{0})d\hat{G}_{0} \end{split}$$

8.3 Symbol Table

8.4 Training Algorithm

Algorithm 1 Training Algorithm

Input: Graph dataset \mathcal{G} , explanation generator g. **Output:** Trained explanation generator g_{α} .

- Initialize explanation generator $g_{\alpha^{(0)}}$. for $t \in epochs$ do 3: for $G \in \mathcal{G}$ do $\hat{G}_0^{(t)} \leftarrow g_{\alpha^{(t)}}(G)$ Prompt Query q_t 4: ← prompting $(G, \hat{G}_0^{(t)})$ into sequence $s_t \leftarrow \phi(q_t)$ $G^{\mathcal{N}} \leftarrow \text{randomly sampled graph noise}$ 6: 7: $\hat{G}^{(t)} \leftarrow s_t \hat{G}_0^{(t)} + (1 - s_t) G^{\mathcal{N}}$ Compute L_{GIB} 10: Update $g_{\alpha^{(t)}}$ with loss back propagation. 11:
- 13: **return** Trained explanation generator g_{α} .

(12)

Symbol Name	Symbol Meaning
G	original to-be-explained graph
Y	prediction label for G
G^*	optimized sub-graph explanation
Y^*	prediction label for G^*
$I(\cdot)$	Mutual Information
\mathcal{V}	Node set
\mathcal{E}	Edge set
X	Feature matrix
A	Adjacency matrix
n	Number of nodes
d	Dimension of feature
i	The i -th node
j	The j -th node
A^{ij}	edge from node i to node j, not used later
\bar{Y}	ground-truth label for graph G
\hat{G}	to-be-explained GNN model
\hat{G}	The sub-graph generated by explainer
\hat{G}_0	The sub-graph generated by original explainer
g_{lpha}	original explainer
g_{eta}'	GNN explainer with LLM embedded
α^*	The parameters of original explainer g_{α}
β^*	The parameters of LLM embedded explainer g'_{β}
ϕ	Large Language Model
λ	Hyper-parameter for the trade-off between size constraint and
	mutual information
$\hat{\mathcal{G}}$	Set of \hat{G}
H	The loss function for GNN explainer
\hat{Y}_0	Prediction Label for \hat{G}_0
\hat{Y}	Prediction Label for \hat{G}
s	LLM score, fitting score, grading
$G^{\mathcal{N}}$	The random noise graph with $G^{\mathcal{N}} \sim \mathcal{N}(0,1)$
Q	The distribution of β
F	Variational energy, proposed by Graves (2011)
$L(\hat{G}, s)$	Network loss, proposed by Graves (2011)
$L^E(\beta,s)$	Error loss, proposed by Graves (2011)
$L^C(\beta,s)$	Complexity loss, proposed by Graves (2011)
$KL(\cdot)$	KL divergence
$L(f, \beta, s)$	Minimum description length form of variational energy
	F(Rissanen, 1978; Graves, 2011)
Δ	The gradient of F toward \hat{G}_0 with $\Delta = \frac{\partial F}{\partial \hat{G}_0}$

Table 3: Important notations and symbols table.